ISBN: 978-3-95450-253-0 ISSN: 2673-5571 doi:10.18429/JACoW-HB2023-TUC3I1

# ULTRA-LOW EMITTANCE BUNCHES FROM LASER COOLED ION TRAPS FOR INTENSE FOCAL POINTS

S. J. Brooks*, Brookhaven National Laboratory, Upton, NY, USA

*Abstract*

Laser-cooled ion traps are used to prepare groups of ions in very low temperature states, exhibiting such phenomena as Coulomb crystallization. This corresponds to very small normalized RMS emittances of $10^{-13}$–$10^{-12}$ m, compared to typical accelerator ion sources in the $10^{-7}$–$10^{-6}$ m range. Such bunches could potentially be focused a million times smaller, compensating for the lower number of ions per bunch. Such an ultra-low emittance source could enable high-specific-luminosity colliders where reduced beam current and apertures are needed to produce a given luminosity. Further advances needed to enable such colliders include linear, helical or ring cooling channel designs for increased bunch number or current throughput. Novel high density focal points using only a single bunch also appear possible, where the high density particles collide with themselves. At collider energies ~100 GeV, these approach the nuclear density and offer a way of studying larger quantities of neutron star matter and other custom nuclear matter in the lab.

## LASER COOLED ION TRAPS

Laser cooling can be applied to ions in any type of trap, for example the Paul trap configuration shown in Fig. 1. This configuration has four AC/RF transverse electrodes powered to produce a quadrupole, with DC longitudinal end caps that are positive like the ions. The rapidly varying transverse electrostatic quadrupole produces an overall dynamic focussing effect on the ions transversely that is analogous to alternating gradient focussing in accelerators.

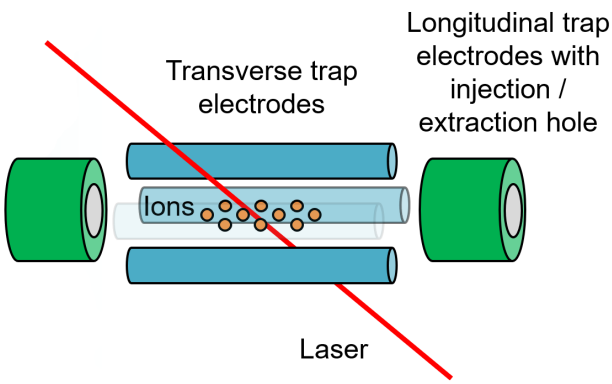


Figure 1: Paul ion trap geometry.

The mechanism of laser Doppler cooling relies on the absorption and subsequent emission of a photon by an allowed transition of the electrons orbiting the ion [1, 2]. One key feature is that the absorbed photons have momentum in the direction of the laser beam, whereas the emitted photons are in random directions, meaning a net force is exerted on the ion. The second required feature is that the transition cross-section has a linewidth that depends on frequency strongly enough that ion travelling towards the laser can be preferentially slowed. A force depending on velocity can act as a non-conservative damping term.

A frequently used example is the $Ca^+$ ion that has a transition around 397 nm with linewidth $\Gamma = 2\pi \times 23$ MHz. The photon itself has a frequency $f = c/397\,\text{nm} = 755$ THz. Comparing the linewidth to this and expressing as a fraction of the speed of light, we would expect the transition to be active over a velocity range of approximately $c(23\,\text{MHz}/755\,\text{THz}) = 9.1$ m/s.

Once the laser is carefully tuned to interact with ions nearly at rest, cooling can proceed. Because of the scattering from re-emission of photons, there is a well-known Doppler cooling limit temperature $T_D = \hbar\Gamma/2k_B = 0.552$ mK here.

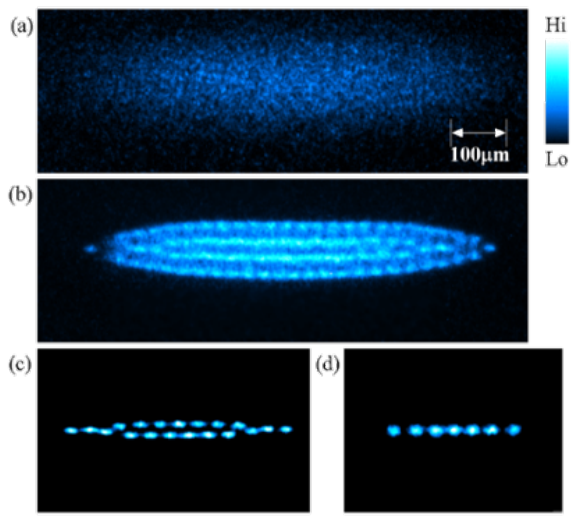


Figure 2: Fluorescence of a Coulomb crystal in the S-POD trap [3] at the University of Hiroshima.

The limiting temperature is so small that the ions can attain the solid 'Coulomb crystal' state where a lattice is held by the balance of repulsive space charge forces and the effective trapping potential. Figure 2 shows an experimental result where the Coulomb crystal structure is made visible by the ion fluorescence (emitted photons from the cooling process).

The hardware required to construct a Paul trap is comparatively simple, with Fig. 3 showing the IBEX trap [4] operated at Rutherford Appleton Laboratory (RAL).

* sbrooks@bnl.gov

ISBN: 978-3-95450-253-0 ISSN: 2673-5571 doi:10.18429/JACoW-HB2023-TUC3I1

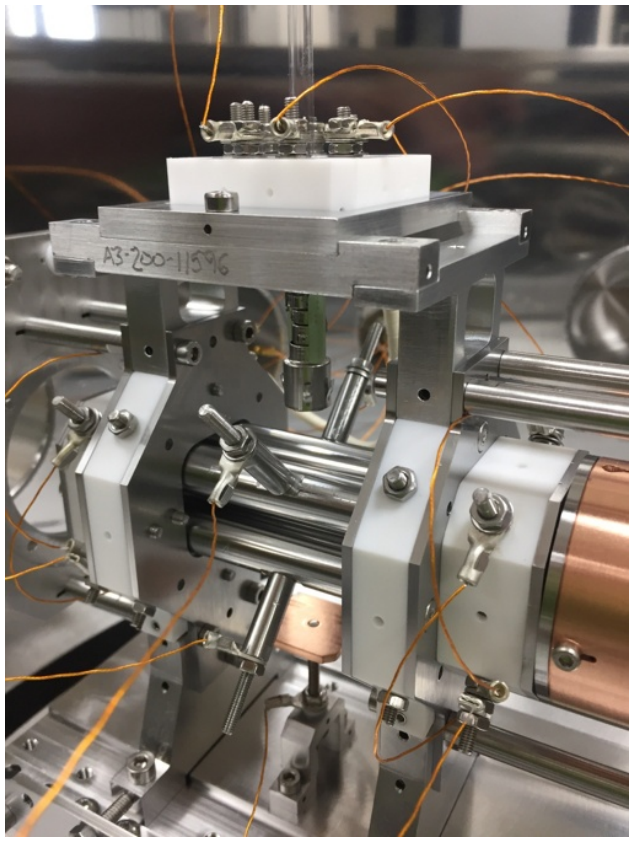

Figure 3: The IBEX Paul trap (RAL) with vacuum chamber opened. The four rods in the center of the image are the transverse trap electrodes.

### *Laser Doppler Cooling Simulation*

A simulation code that runs on the GPU using OpenCL has been written to simulate the ion trap. 4th order Runge–Kutta steps in the trap potential are interleaved with pairwise space charge kicks. The ions have a ground and an excited state, the transitions between them being governed by a statistical model whose rates agree with the quantum description of a two-level atom in a laser beam. These excitations and de-excitations come with appropriate $\Delta p = \hbar k$ momentum kicks, where it is important to apply the events at truly random points within each time-step, so the short periods where the Doppler process is active are not jumped over.

The results of such a simulation are shown in Fig. 4, where the eventual configuration of ions was a long thin Coulomb crystal several ions wide. Two phases of cooling can be seen: the first occurs before formation of a solid Coulomb crystal core from the initially gas-like ions, while the second ends when the small fraction of remaining ions 'orbiting' the solid core eventually lose enough momentum to merge with it. The final temperature is a small multiple of the predicted Doppler limit. The RF nature of the transverse focussing means some vibrations can be excited that take the temperature above the limit.

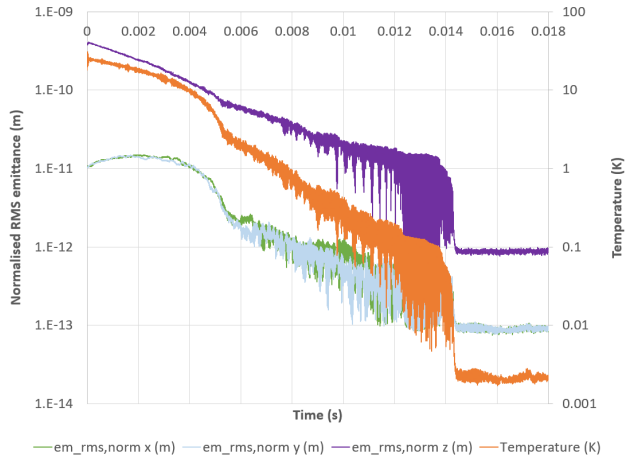


Figure 4: Laser Doppler cooling simulation with $N = 500$ ions.

### *Ion Trap Flexibility*

Laser cooled ion traps are flexible sources with several bunch parameters that can be varied over a wide range:-

- Bunch charge, via gas pressure and trap voltage. IBEX has trapped $10^6$–$10^7$ ions [5] and S-POD has seen anything from single ions up to $10^7$ [6].
- Bunch size, shape and aspect ratio, via trap voltages, geometry and collimation. The trap electrode configurations may be easily exchanged once the rest of the experiment (diagnostics, signal generators) is set up.
- Emittance and temperature, by stopping cooling part way or tightening the trap. As the ions are non-relativistic, their emittance at the Doppler cooling limit is given to a good approximation by

$$\epsilon_{\mathrm{norm,rms}} \simeq \frac{\sigma_x \sigma_v}{c} = \frac{\sigma_x}{c}\sqrt{\frac{k_B T_D}{m}} = \frac{\sigma_x}{c}\sqrt{\frac{\hbar\Gamma}{2m}}.$$

  By tightening the trap, it is also possible to achieve the quantum emittance limit, which for a single ion is

$$\epsilon_{\mathrm{norm,rms}} \geq \frac{\hbar}{2mc}.$$

- Other ion species can be cooled via *sympathetic cooling*, in which a coolable ion (e.g., $^{40}Ca^+$) is mixed in thermal contact with the desired species in the trap [7].

One example of this flexibility is shown in Fig. 5, where the transverse trapping voltages were made much smaller than the longitudinal ones, giving a Coulomb crystal that is only one or two ions thick in the longitudinal direction.

## LOWER BOUNDS ON FOCAL SIZE

The cooled bunch from the ion trap has a very small $\sigma_v$ but a macroscopic size. One can consider rotating its

ISBN: 978-3-95450-253-0 ISSN: 2673-5571 doi:10.18429/JACoW-HB2023-TUC3I1



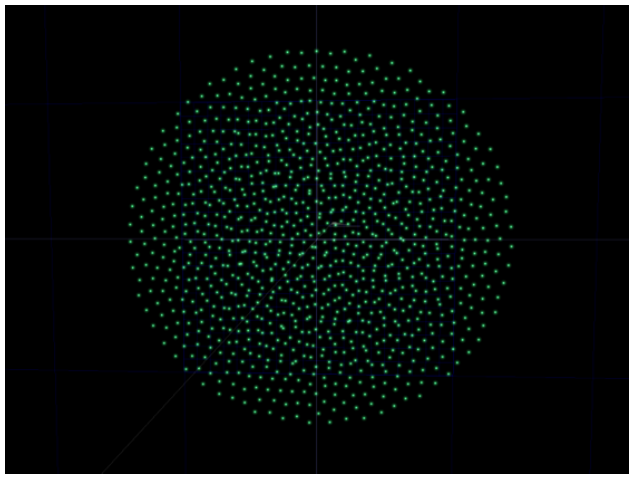

Figure 5: 2D Coulomb crystal that can be created by an anisotropic trap.

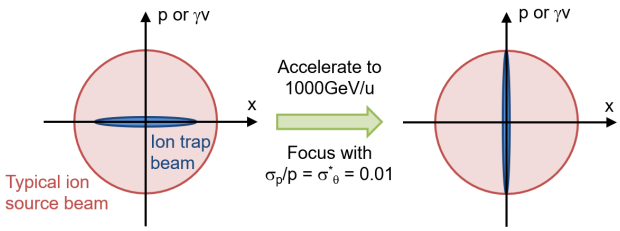


Figure 6: Rotation of phase space.

phase space in a focussing system, analogous to a collider interaction point, as shown in Fig. 6.

The parameters of the ion trap bunch are compared to those of a more conventional ion source (e.g., [8]) in Table 1.

Table 1: Comparison of Bunch Parameters

| Parameter | Ion source | Ion trap |
|---|---|---|
| $N$ | $10^9$ | 500 |
| $\epsilon_{\text{norm,rms}}$ | $10^{-7}$ m | $2 \times 10^{-13}$ m |
| Initial condition: | | |
| $\sigma_x$ | 1 mm | 90 µm |
| $\sigma_v$ | 30 km/s | 0.65 m/s |
| $T$ | 4.3 MK | 2 mK |
| At focus: | | |
| $\sigma_x^*$ | 9.4 nm | 18 fm |
| $\sigma_\theta^*$ | 10 mrad | 10 mrad |
| $L$/bunch | $9 \times 10^{28}$ cm$^{-2}$ | $6 \times 10^{27}$ cm$^{-2}$ |

It can be seen that the ion trap bunch can be focussed far smaller than the conventional bunch, albeit with a lower population of particles. To compare these in a like-for-like fashion, the luminosity per bunch has also been calculated via

$$L = \frac{N_1 N_2 f N_b}{4\pi\sigma_x\sigma_y} \quad \Rightarrow \quad L/\text{bunch} = \frac{N_1 N_2}{4\pi\sigma_x\sigma_y}.$$

While the ion trap bunch produces less luminosity in an absolute sense, the 'specific luminosity', or luminosity per particle is 130,000 times higher than with the conventional bunch, which suggests this could be a route to highly energy efficient colliders. The scaling direction towards high specific luminosity can be defined as follows. Luminosity is held constant if $N \propto \sigma^*$ and if $\sigma_\theta^*$ at the interaction point is also held constant, this becomes $N \propto \sigma^* \propto \epsilon$. As $N$ is decreased, the luminosity can be maintained as long as $\sigma^*$ and emittance are decreased in proportion.

In fact, the ion trap collision above will saturate the cross section if $\sigma_{tot} > 84$ mbarn, in which case the expected number of collisions per crossing $\sigma_{tot}(L/\text{bunch})$ is greater than the 500 ions in each bunch. This means that after one pass, the bunch is gone!

### *Longitudinal Plane Focussing*

Such a small value of $\sigma^*$ will require the longitudinal bunch length to also be short. The ion trap can produce an equally small emittance in all three planes, so we will search for focussing systems that can *focus in all three planes* to some extent. Although relativity makes focussing longitudinally at high $\gamma$ more difficult.

Additionally, the high spatial density of the focussed bunch raises the question of whether space charge repulsion limits the minimum size before emittance does. This will also be examined.

### *Spherical Bunch Model*

A simple model of a three dimensional focus is an imploding sphere of charge in the bunch rest frame. If the inward kinetic energy at the outer surface of the bunch is initially $E_{k,in}$ in its rest frame, then the space charge radius limit is

$$r \geq \frac{1}{4\pi\epsilon_0}\frac{Nq^2}{E_{k,in}},$$

where $q$ is the charge of a single ion. This gives density scaling as $\rho \propto N/r^3 \propto E_{k,in}^3/N^2$.

Emittance produces another limit

$$\sigma_x \geq \frac{\epsilon_{\text{norm,rms}}}{\sigma_{\beta\gamma}},$$

where $\sigma_{\beta\gamma}$ is the RMS $\beta\gamma$ in the bunch rest frame. These RMS quantities may be related to total radii etc. via

$$\sigma_x = r/\sqrt{5}, \qquad \sigma_{\beta\gamma} = (\beta\gamma)_{in}/\sqrt{5}.$$

The Lorentz transformation from the lab frame where the bunch momentum spread is $\sigma_p/p$ gives

$$\sigma_{\beta\gamma,\text{Transv.}} = (\beta\gamma)_{\text{beam}}\sigma_\theta^*, \qquad \sigma_{\beta\gamma,\text{Long.}} = \beta_{\text{beam}}\sigma_p/p,$$

where $(\beta\gamma)_{\text{beam}}$ is proportional to the average beam momentum and $\sigma_{\beta\gamma}$ is assumed to be small relative to this.

ISBN: 978-3-95450-253-0 ISSN: 2673-5571 doi:10.18429/JACoW-HB2023-TUC3I1

### *Additional Complexities*

Once the nuclei are within each others' electron clouds, $Ca^+$ will start to behave more like fully-stripped $Ca^{20+}$ as charge shielding from the electrons is reduced.

The longitudinal focussing being different implies the charge distribution in the bunch rest frame may be a non-spherical ellipsoid. The space charge forces in such an ellipsoid are still linear but coupled between the planes just like the 2D KV envelope equations. In the following sections, the approach taken is to integrate backwards from focal point and fit the focal ellipsoid size to match the incoming $\sigma_\theta^*$ and $\sigma_p/p$.

### *Energy Scaling*

Figure 7 shows the emittance and space charge limits on focal size for ion trap bunches accelerated to between 1 eV/u and 1 TeV/u. This is for $N$ = 500 ions with $\sigma_p/p$ = $\sigma_\theta^*$ = 0.01. The plot also shows the resulting bunch density; for reference, water is $10^3$ kg/m$^3$ and the nuclear density is $2.5 \times 10^{17}$ kg/m$^3$. The discontinuity in the space charge and density lines is when the calculation switches from using $Ca^+$ to fully-stripped ions (nuclei).

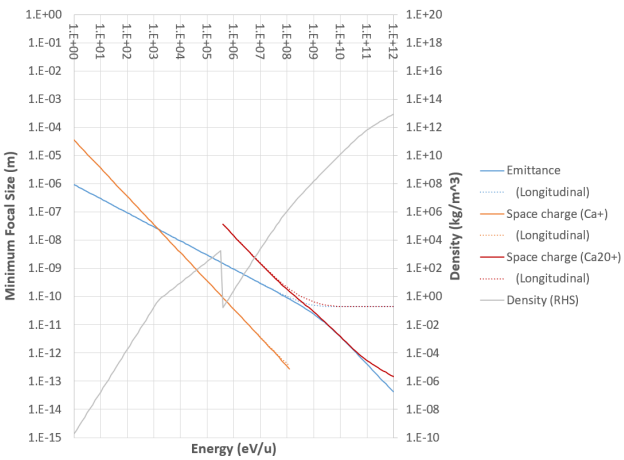


Figure 7: Focal size and density as a function of energy.

This first example doesn't quite get to the nuclear density, mainly because of the longitudinal size being larger, so Fig. 8 shows how adjusted parameters can achieve this. This still has $N$ = 500 ions but $\sigma_p/p$ and $\sigma_\theta^*$ are doubled to 0.02. The main change is that the trap is made 20× smaller using tighter electric fields, so overall emittances are also reduced 20-fold. The trap is also slightly anisotropic with $\epsilon_L = 1.9\epsilon_T$.

Other ways of increasing the longitudinal focussing could include colliding bunches, so the longitudinal momentum difference is larger, or using a fixed-field accelerator (FFA) focussing channel with a very wide dp/p range.

### *Potential Future Applications*

Aligning a focus to within $10^{-14}$ m will require very precise positional control, but this technology has continued to improve. Atomic-level positioning was available in the 1980s and mirrors for gravitational wave observatories [9]

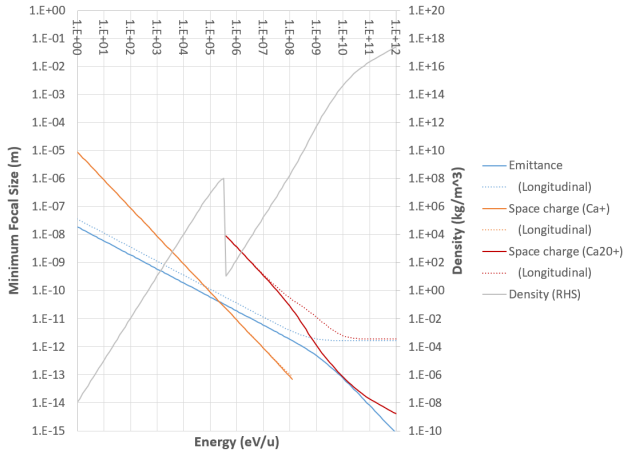


Figure 8: Focal size and density as a function of energy, with 20 times smaller initial emittance and twice the energy spread.

have been controlled to almost the nuclear size. Alignment errors must be read back in order to drive a high-accuracy feedback system. The distribution of ions scattered from the interaction point contains extremely high-resolution data, as the outgoing angles change on scales similar to the focal size itself. Intense focal points provide a way of using positional stability, together with the ultra-low emittance from the ion trap, to produce a physically new configuration.

The low emittance from the ion trap represents a low entropy initial state for any experiment done with the ions, improving experimental control. The high densities of the focal point allow investigation of white dwarf or neutron star matter, while the nuclear-level positional control allows 3-way and multi-way particle collisions to be constructed. Synthesis of custom shapes of nuclear matter and possible neutron-rich superheavy elements are also enabled by these techniques.

## FOCUSSING BEAMLINE OPTIMISATION

Assuming suitably stable electromagnetic fields are available, is there anything besides the emittance and space charge limits already discussed that could prevent the formation of an intense focus? One possibility is that optical aberrations in the focussing system (lens nonlinearity, spherical aberration, chromaticity etc.) could prevent formation of such a small focus, or that focussing to a small size in all three dimensions at once is not allowed dynamically. The following study finds beamlines that solve both of these issues.

In this test, an ion trap distribution of $N$ = 20000 ions at a temperature of $T$ = 2 mK were given an energy chirp and injected into a curved electrostatic beamline. The energy chirp is necessary to increase $\sigma_{\beta\gamma,\mathrm{Long.}}$ for better longitudinal focussing. The beamline consists of 15 rings of 12 point-charge 'electrodes', so each ring can form a generalised electrostatic multipole lens. Also the beamline bends through a 135° angle to better couple the longitudinal plane to the transverse focussing of the lenses.

ISBN: 978-3-95450-253-0 ISSN: 2673-5571 doi:10.18429/JACoW-HB2023-TUC3I1



### *Optimisation of Electrode Voltages*

An optimiser was allowed to change all the electrode charges, with constraints that a ring can not have an overall monopole charge (accelerating or decelerating). The energy chirp was also allowed to be varied, for a total of $15(12-1)+1 = 166$ parameters. The optimiser goal was to minimise focal size by minimising all output ion displacements at a particular finish time.

A modified Levenburg–Marquardt method with nonlinearity correction [10] was created to more rapidly optimise in this case with a wide range of parameter sensitivities plus some nonlinearity. Figure 9 shows the improvement from adding higher-order correction terms beyond the first order LM step.

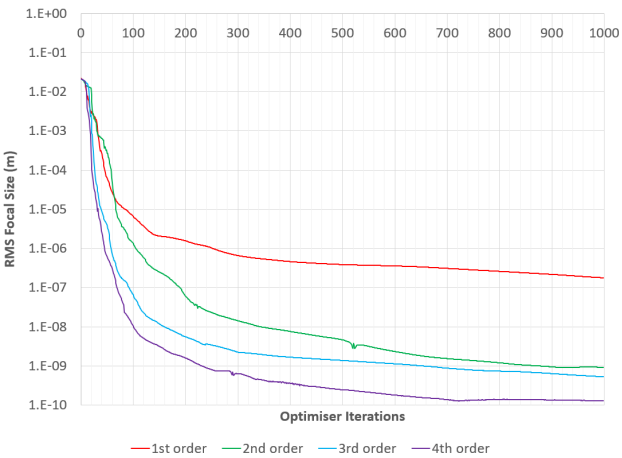


Figure 9: Improvement of Levenburg–Marquardt optimiser when higher-order correction terms are added.

### *Results*

Figure 10 shows the minimum focal sizes achieved for a range of bunch energies as the number of electrode rings is varied. The values are limited by the normalised emittance which is constant but corresponds to a smaller geometrical emittance for higher energies. The dp/p chirp also provides a limit: larger dp/p allows a smaller minimum focal size but at the cost of larger higher-order aberrations, which the electrostatic lenses must cancel. Thus, as the number of lenses is increased, higher dp/p values and smaller focal sizes can be achieved using a more complex beamline.

The "T=0" line on Fig. 10 shows the size limit from pure optical aberrations, in the case of zero initial emittance. Beyond around five lenses and $< 10^{-10}$ m focal size, it appears to hit a numerical noise floor from the double precision arithmetic. The points labelled "theory" show the minimum allowed size calculated analytically from the emittance and dp/p chirp. The real results from the optimised beamline generally track closely above these lower bounds, showing good convergence.

The decrease of focal size with energy is plotted in Fig. 11. Here, the points for one or two electrode rings are seen to stop decreasing, while those for more lenses generally track

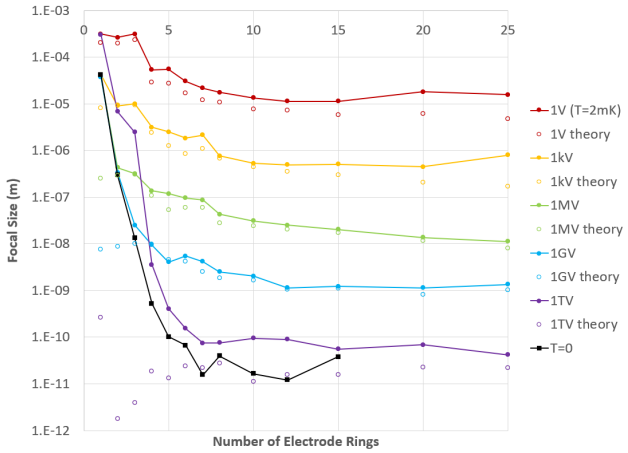


Figure 10: Focal Size vs. Electrodes Used.

with the theoretical minimum for 1% dp/p chirp. Although for the highest energies this chirp value is not achieved, either through hitting numerical noise or the bunch geometrical emittance already being very small.

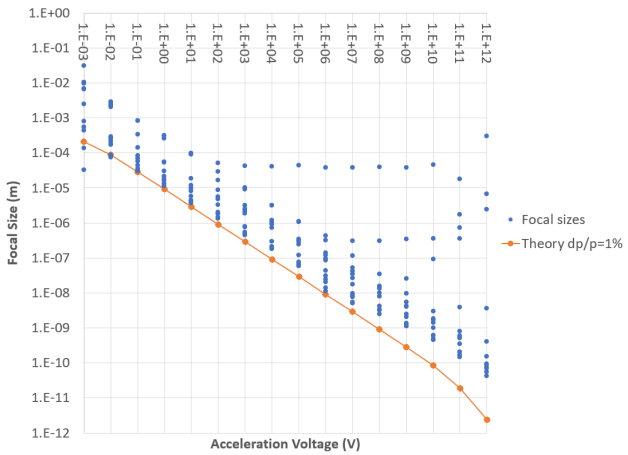


Figure 11: Focal Size vs. Energy.

The chirp chosen for each energy and number of electrode rings is shown in Fig. 12. As more beamline elements are allowed, the optimiser can cancel aberrations for a larger momentum range, leading to a higher chosen chirp.

Finally, Fig. 13 plots the focal size directly against the chosen chirp values, highlighting how the theoretical minimum focal size shrinks with increasing chirp and how the optimised results generally track with this, ignoring the 1 TeV/u case that has some trouble with numerical noise.

## ALTERNATIVE SCHEMES

### *Cooling at High Energy?*

Doppler cooling also works in a boosted frame, so perhaps ions can be cooled in a ring instead of a static trap. Coulomb crystals have been produced this way by the PALLAS ring [11], but with a beam velocity of only 2.8 km/s. A table of additional cooled ion ring examples is given in [12].

ISBN: 978-3-95450-253-0 ISSN: 2673-5571 doi:10.18429/JACoW-HB2023-TUC3I1

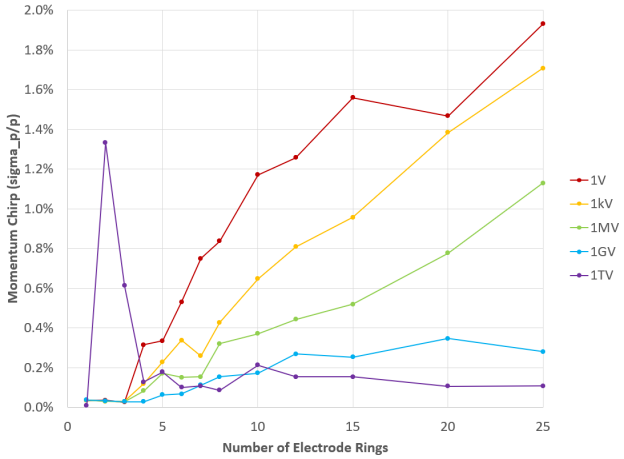


Figure 12: Optimal Chirp vs. Electrodes Used.

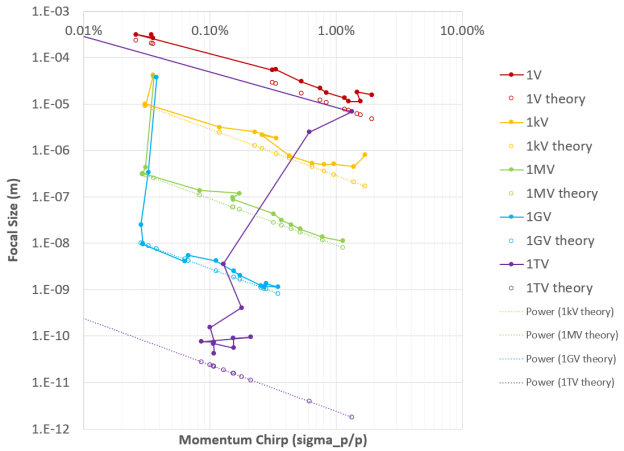


Figure 13: Focal Size vs. Initial Chirp.

The advantages of cooling in a ring are: creation of cold beams at or near final energy; and bypassing jitter from the RF acceleration process. The blue-shift of the laser beam can also be used to cool using harder transitions, which improves cooling rate but increases limiting temperature.

The disadvantages of cooling in a ring are: it needs a special low-intra-beam-scattering (IBS) ring lattice with very low phase advance per cell, in which the bunch velocity distribution must be kept near-Maxwellian; too high an energy or magnetic field could strip the ions; and a ring is more expensive than a static ion trap.

### *Increasing Current Throughput*

The throughput of the basic ion trap is not very high because the cooling process takes 16 ms as shown in Fig. 4. This would produce $10^7$ ions every 16 ms (62.5 Hz), for an average current of 100 pA.

However, the trap is small enough and the cooling time short enough that a linear CW cooling channel could be made at a PALLAS-like speed of 50 km/s. This would contain bunches every 100 ns (10 MHz), spaced by 5 mm. The channel would be 16 ms*50 km/s = 800 m long but could be coiled up since the trap is narrow with rod electrodes only a few mm apart. The average current from this channel could go as high as $10^{14}$ ions per second, or 16 µA.

## CONCLUSION AND FUTURE WORK

Ultra-low emittance bunches provide some interesting unexplored regimes in accelerators. They have $10^6$ times smaller emittance than conventional bunches and optical manipulation of such bunches in an accelerator beamline has not yet been tried.

Lower-entropy initial states are likely to be the long term trend as experiments improve and ultra-low emittance bunches are an example of this. The positional quantum ground state can also be achieved, which is the basis for ion trap quantum computing, but also means entangled states (e.g., spins) could be produced in an accelerator beam. Ultimately, it appears custom synthesis of nuclear density matter is allowed by using such a small initial emittance in conjunction with very high-stability focussing system at energies around 1 TeV/u.

### *Recent Funding at BNL*

The author has recently received Lab-Directed R&D (LDRD) funding from BNL, to investigate ion traps and construct the basic foundational ion trap system shown in Fig. 14. This funding is a total of $400k including overheads over the two years from October 2023 to September 2025. Probably these funds will not be enough to add laser cooling but instead just demonstrate ion trapping.

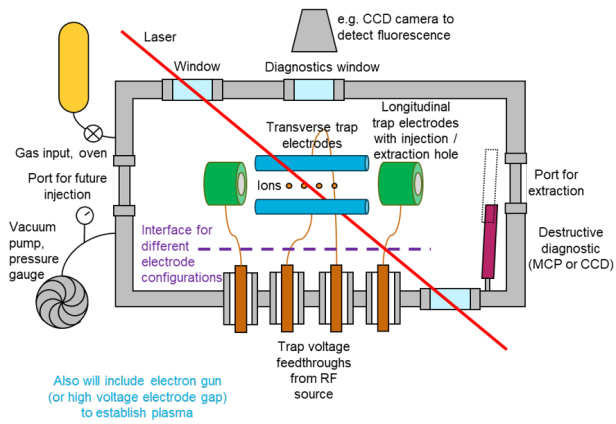


Figure 14: Schematic of ion trap system.

## ACKNOWLEDGEMENTS

The author would like to thank David Kelliher from the IBEX ion trap at BNL and Hiromi Okamoto who developed the S-POD ion trap at Hiroshima University, for their helpful discussions and technical advice.

ISBN: 978-3-95450-253-0 ISSN: 2673-5571 doi:10.18429/JACoW-HB2023-TUC3I1

## REFERENCES


[1] A. Steane, "The ion trap quantum information processor", *Appl. Phys. B*, vol. 64, pp. 623–642, 1997. doi:10.1007/s003400050225

[2] H. J. Metcalf and P. van der Straten, "Laser Cooling and Trapping of Neutral Atoms", *The Optics Encyclopedia*, vol. 38, pp. 847–853, 2007. doi:10.1002/9783527600441.oe005

[3] K. Izawa, K. Ito, H. Higaki and H. Okamoto, "Controlled Extraction of Ultracold Ions from a Linear Paul Trap for Nanobeam Production", *J. Phys. Soc. Japan*, vol. 79, p. 124502, 2010. doi:10.1143/JPSJ.79.124502

[4] S. L. Sheehy *et al.*, "Commissioning and First Results of the IBEX Paul Trap", in *Proc. IPAC'17*, Copenhagen, Denmark, May 2017, pp. 4481–4484. doi:10.18429/JACoW-IPAC2017-THPVA027

[5] L. K. Martin, S. Machida, D. J. Kelliher, S. L. Sheehy, "A study of coherent and incoherent resonances in high intensity beams using a linear Paul trap", *New J. Phys.*, vol. 21, p. 053023, 2019. doi:10.1088/1367-2630/ab0e28

[6] R. Takai, H. Enokizono, K. Ito, Y. Mizuno, K. Okabe and H. Okamoto, "Development of a Compact Plasma Trap for Experimental Beam Physics", *Japan. J. Appl. Phys.*, vol. 45, pp. 5332–5343, 2006. doi:10.1143/JJAP.45.5332

[7] K. Muroo, H. Okamoto, N. Miyawaki and Y. Yuri, "Simulation study of ultrahigh-precision single-ion extraction from a linear Paul trap", *Prog. Theor. Exp. Phys.*, vol. 2023, p. 063G01, 2023. doi:10.1093/ptep/ptad071

[8] S. A. Kondrashev, A. Barcikowski, B. Mustapha, P. N. Ostroumov, and N. Vinogradov, "Emittance Measurements of Ion Beams Extracted from the High-Intensity Permanent Magnet ECR Ion Source", in *Proc. ECRIS'08*, Chicago, IL, USA, Sep. 2008, paper THCO–A01, pp. 199–203.

[9] LIGO Scientific Collaboration (August 2014 LSC author list), "Advanced LIGO", 2014. doi:10.48550/arXiv.1411.4547

[10] S. J. Brooks, "Higher-Order Corrections to Optimisers based on Newton's Method", 2023. doi:10.48550/arXiv.2307.03820

[11] U. Schramm, T. Schätz, M. Bussmann and D. Habs, "The quest for crystalline ion beams", *Plasma Phys. Control. Fusion*, vol. 44, pp. B375-–B387, 2002. https://api.semanticscholar.org/CorpusID:13943591

[12] A. Noda *et al.*, "Ultralow Emittance Beam Production based on Doppler Laser Cooling and Coupling Resonance", in *Proc. IPAC'14*, Dresden, Germany, Jun. 2014, pp. 28–33. doi:10.18429/JACoW-IPAC2014-MOZA01